Canonical interpretation of the $D_{s0}(2590)^+$ resonance

Zhuo Gao,[1] Guan-Ying Wang,[1,*] Qi-Fang Lü,[2,3,4,†] Jingya Zhu,[1] and Gao-Feng Zhao[1,‡]

[1]*Joint Research Center for Theoretical Physics, School of Physics and Electronics, Henan University, Kaifeng 475004, China*
[2]*Department of Physics, Hunan Normal University, Changsha 410081, China*
[3]*Synergetic Innovation Center for Quantum Effects and Applications (SICQEA), Changsha 410081, China*
[4]*Key Laboratory of Low-Dimensional Quantum Structures and Quantum Control of Ministry of Education, Changsha 410081, China*

(Received 7 January 2022; accepted 5 April 2022; published 29 April 2022)

The $D_{s0}(2590)^+$ resonance observed by LHCb Collaboration is a strong candidate of the $D_s(2^1S_0)$ state according to its spin parity and strong decay mode. However, the measured mass seems relatively lower than the previous theoretical predictions, which interests the coupled channel interpretations in the literature. In this work, we adopt an alternate approach, taking into account the screening effects in the potential model, to describe the $D_{s0}(2590)^+$ resonance. The mass spectrum and strong decays of the excited charmed-strange mesons are investigated within the modified relativized quark model and $^3P_0$ model. The calculated mass and width of the $D_{s0}(2590)^+$ are consistent with the experimental observations, which indicate that it can be reasonably interpreted as the $D_s(2^1S_0)$ state.

DOI: 10.1103/PhysRevD.105.074037

I. INTRODUCTION

A heavy-light meson is composed of one heavy quark and one light antiquark, and acts as a hydrogen atom. Understanding the heavy-light meson spectrum and searching for the missing resonances are important tasks in hadronic physics, which provide us a good opportunity to deepen our understanding of the complicated nonperturbative behavior of QCD in the low energy regime. Among them, the charmed-strange sector is particularly interesting and has gained wide attention [1–31], since the mysterious $D_{s0}^*(2317)$ and $D_{s1}(2460)$ states observed by *BABAR* and CLEO Collaborations [32,33] have rather lower masses compared with the theoretical predictions in conventional quark models [1–8].

From the Review of Particle Physics [34], there exist twelve states in the charmed-strange sector. The D_s and D_s^* are the ground states, and $D_{s1}(2536)$ and $D_{s2}^*(2573)$ can be well understood as the $P-$wave states. The $D_{s1}^*(2700)$, $D_{s1}^*(2860)$, and $D_{s3}^*(2860)$ can be assigned as the $D_s(2^3S_1)$, $D_s(1^3D_1)$, and $D_s(1^3D_3)$ states, respectively, where the $2S-1D$ mixing effect may be also significant for the vector mesons. The canonical interpretations of $D_{s0}^*(2317)$ and $D_{s1}(2460)$ are problematic in the traditional quark model, while the $X_0(2900)$ and $X_1(2900)$ observed by LHCb Collaboration are undoubtedly exotic [35,36]. Moreover, information on the $D_{sJ}(3040)$ state is quite limited, which prevents us to reach a definite conclusion. It can be seen that the low-lying charmed-strange spectrum is far from being established.

Recently, the LHCb Collaboration observed a new excited resonance $D_{s0}(2590)^+$ in the $D^+K^+\pi^-$ mass distribution of the $B^0 \to D^-D^+K^+\pi^-$ decay [37]. Its mass, width, and spin parity are determined to be $m = 2591 \pm 6 \pm 7$ MeV, $\Gamma = 89 \pm 16 \pm 12$ MeV, and $J^P = 0^-$, respectively. Based on these properties, the LHCb Collaboration suggested that this state is a strong candidate for the radial excited $D_s(2^1S_0)$ state. However, the measured mass seems relatively lower than the previous theoretical predictions in the literature [1–8], which leads to different interpretations on the theoretical side. In Ref. [12], the authors investigated the mass and width of $D_{s0}(2590)^+$ by solving the Bethe-Salpeter equation, and concluded that it can be hardly explained as $D_s(2^1S_0)$ state. Within the semirelativistic potential model and chiral quark model, the mass and width of $D_{s0}(2590)^+$ are not consistent with that of the $D_s(2^1S_0)$ state [8]. In Ref. [13], the authors employ the unquenched quark model to describe the mass of $D_{s0}(2590)^+$ by considering the mixture of the $D_s(2^1S_0)$

*Corresponding author.
wangguanying@henu.edu.cn
†Corresponding author.
lvqifang@hunnu.edu.cn
‡Corresponding author.
10110094@vip.henu.edu.cn

state and D^*K component. Also, the authors performed a coupled-channel calculation including the $D^{(*)}K^{(*)}$, $D_s^{(*)}\omega$ and $D_s^{(*)}\eta$ channels, and found that the $D_{s0}(2590)$ can be regarded as a bare $D_s(2^1S_0)$ state plus dominant D^*K part [14]. These theoretical works suggest that the $D_{s0}(2590)^+$ may be not a pure $D_s(2^1S_0)$ state and the D^*K component should be significant.

Based on the $SU(3)$ light quark flavor symmetry, the $P-$wave charmed-strange mesons is supposed to be higher than their charmed partners. The violation of $SU(3)$ flavor symmetry for $D_{s0}^*(2317)$ and $D_{s1}(2460)$ resonances suggest that they are not pure $P-$wave $c\bar{s}$ states and the coupled-channel effects are essential. Actually, in the literature, the coupled-channel approach, meson-loop effects, or the unquenched quark model has been widely discussed in the charmed-strange sector to reduce the theoretically predicted masses [13–27], which mainly focused on the $D_{s0}^*(2317)$ and $D_{s1}(2460)$ resonances. However, the situation of the $D_{s0}(2590)^+$ is better. The mass gap between $D_{s1}^*(2700)$ and $D_{s0}(2590)$ is

$$m[D_{s1}^*(2700)] - m[D_{s0}(2590)] = 123\ \text{MeV}, \qquad (1)$$

and the mass gap between two $2S$ charmed states $D_1^*(2600)$ and $D_0(2550)$ with the latest measurements of LHCb Collaboration is [38]

$$m[D_1^*(2600)] - m[D_0(2550)] = 124\ \text{MeV}. \qquad (2)$$

The approximately equal mass splittings of charmed and charmed-strange sectors strongly suggest that the $D_{s0}(2590)$ should be the partner of $D_0(2550)$ and can be assigned as the $D_s(2^1S_0)$ state as the LHCb Collaboration suggested.

Instead of the unquenched approaches with higher Fock states, the potential model including screening effects is an alternate approach to lower the mass spectrum, which has been extensively employed to study the properties of conventional mesons and achieved significant success. The advantage of the screening potential is that one can bring down the masses of excited states while avoiding involving higher Fock components. Hence, we expect that the potential model including screening effects may relieve the tension between measured mass and theoretical predictions under the assignment of $D_{s0}(2590)$ as $D_s(2^1S_0)$ state. Moreover, it is natural and necessary to explore the possible conventional descriptions for a newly observed particle before introducing more complicated and exotic configurations. In this work, we apply the Godfrey-Isgur's relativized quark model including screening effects to revisit the mass spectrum of the charmed-strange mesons, and then adopt the obtained wave functions to study their strong decay behaviors in the $^3P_0$ model. Our results show that the calculated mass and width of the $D_{s0}(2590)^+$ are consistent with the experimental observations, which suggest that it can be reasonably interpreted as the $D_s(2^1S_0)$ state.

This article is organized as follows. In Sec. II, we briefly introduce the relativized quark models and $^3P_0$ models. The results and discussions of charmed-strange mesons are presented in Sec. III. Finally, a summary is given in the last section.

II. MODELS

A. The relativized quark model

In this subsection, we will give a brief introduction of the relativized quark model proposed by Godfrey and Isgur (GI model) [1]. This model has been extensively adopted to investigate the properties of conventional hadrons [1,7,28,39–44] and tetraquarks [45–55], and give a unified description of different flavor sectors. In particular, for the low-lying states, the relativized quark model plays an important role in studying their mass spectra and provides an effective criterion to distinguish conventional mesons from exotics.

For a two-body system, the relevant Hamiltonian can be written as

$$H = H_0 + V^{\text{oge}} + V^{\text{conf}}, \qquad (3)$$

where

$$H_0 = \sqrt{p^2 + m_1^2} + \sqrt{p^2 + m_2^2} \qquad (4)$$

is the relativistic kinetic energy, V^{oge} is the one gluon exchange potential, and V^{conf} corresponds to the confining potential. The induced spin-the smearing transformation, one has the V^{oge} and V^{conf}.

More explicitly, the potentials V^{oge} and V^{conf} can be expressed as

$$\begin{aligned} V^{\text{oge}} = {} & \beta_{12}^{1/2}\tilde{G}(r)\beta_{12}^{1/2} + \delta_{12}^{1/2+\epsilon_c}\frac{2\boldsymbol{S_1}\cdot\boldsymbol{S_2}}{3m_1m_2}\nabla^2\tilde{G}(r)\delta_{12}^{1/2+\epsilon_c} + \delta_{12}^{1/2+so(v)}\frac{(\boldsymbol{S_1}+\boldsymbol{S_2})\cdot\boldsymbol{L}}{m_1m_2}\frac{1}{r}\frac{\partial\tilde{G}(r)}{\partial r}\delta_{12}^{1/2+so(v)} \\ & + \delta_{11}^{1/2+so(v)}\frac{\boldsymbol{S_1}\cdot\boldsymbol{L}}{2m_1^2}\frac{1}{r}\frac{\partial\tilde{G}(r)}{\partial r}\delta_{11}^{1/2+so(v)} + \delta_{22}^{1/2+so(v)}\frac{\boldsymbol{S_2}\cdot\boldsymbol{L}}{2m_2^2}\frac{1}{r}\frac{\partial\tilde{G}(2)}{\partial r}\delta_{22}^{1/2+so(v)} \\ & + \delta_{12}^{1/2+\epsilon_t}\left(\frac{\boldsymbol{S_1}\cdot\hat{\boldsymbol{r}}\boldsymbol{S_2}\cdot\hat{\boldsymbol{r}}-\boldsymbol{S_1}\cdot\boldsymbol{S_2}/3}{m_1m_2}\right)\left(\frac{1}{r}\frac{\partial}{\partial r}-\frac{\partial^2}{\partial r^2}\right)\tilde{G}(r)\delta_{12}^{1/2+\epsilon_t}, \end{aligned} \qquad (5)$$

and

$$V^{\mathrm{conf}} = \tilde{S}(r) - \delta_{11}^{1/2+so(s)} \frac{\boldsymbol{S_1}\cdot\boldsymbol{L}}{2m_1^2}\frac{1}{r}\frac{\partial\tilde{S}(r)}{\partial r}\delta_{11}^{1/2+so(s)} - \delta_{22}^{1/2+so(s)} \frac{\boldsymbol{S_2}\cdot\boldsymbol{L}}{2m_2^2}\frac{1}{r}\frac{\partial\tilde{S}}{\partial r}\delta_{22}^{1/2+so(s)}. \tag{6}$$

Here, the $\tilde{G}(r)$ and $\tilde{S}(r)$ are the smeared potentials, and can be written as

$$\tilde{G}(r) = -\sum_{k=1}^{3}\frac{4\alpha_k}{3r}\mathrm{erf}(\tau_{k12}r) \tag{7}$$

and

$$\tilde{S}(r) = br\left[\frac{e^{-\sigma_{12}^2 r^2}}{\sqrt{\pi}\sigma_{12}r} + \left(1+\frac{1}{2\sigma_{12}^2 r^2}\right)\mathrm{erf}(\sigma_{12}r)\right] + c \tag{8}$$

with

$$\frac{1}{\tau_{k12}^2} = \frac{1}{\gamma_k^2} + \frac{1}{\sigma_{12}^2} \tag{9}$$

and

$$\sigma_{12}^2 = \sigma_0^2\left[\frac{1}{2}+\frac{1}{2}\left(\frac{4m_1m_2}{(m_1+m_2)^2}\right)^4\right] + s^2\left(\frac{2m_1m_2}{m_1+m_2}\right)^2. \tag{10}$$

The definition of δ_{11}, δ_{12}, δ_{22}, and β_{12} are

$$\delta_{ij} = \frac{m_im_j}{(p^2+m_i^2)^{1/2}(p^2+m_j^2)^{1/2}} \tag{11}$$

and

$$\beta_{12} = 1 + \frac{p^2}{(p^2+m_1^2)^{1/2}(p^2+m_2^2)^{1/2}}. \tag{12}$$

The p is the magnitude of the relative momentum between the quark and antiquark. The m_1 and m_2 are masses of the quark and antiquark, respectively. The $\alpha_k, \gamma_k, b, c, \sigma_0, s$ and ϵ_i are the parameters introduced in the relativized quark model.

B. Screened potential

For high excited states, it is necessary to introduce the screening effects to the relativized model, because the linear confining potential will be screened and softened by the vacuum polarization effects at a large distance [56–58]. Also, the modified relativized model (MGI model) including screen effects turns out to be able to give a better description of the mass spectra for the radial and orbital excitations [29,49,59–64].

To incorporate the screen effects in the relativized quark model, we should replace the confining potential $\tilde{S}(r)$ with a screened potential. The $\tilde{S}(r)$ actually arises from the linear confinement according to the smearing transformation. For an arbitrary potential $f(r)$, the smeared ones $\tilde{f}(r)$ can be expressed as

$$\tilde{f}(r) = \int d^3r'\rho_{12}(\mathbf{r}-\mathbf{r}')f(r') \tag{13}$$

with

$$\rho_{12}(\mathbf{r}-\mathbf{r}') = \frac{\sigma_{12}^3}{\pi^{3/2}}e^{-\sigma_{12}^2(\mathbf{r}-\mathbf{r}')^2}. \tag{14}$$

It can be noticed that the linear confining potential $S(r) = br + c$ indeed leads to the $\tilde{S}(r)$ through the above smearing transformation. Here, the constant c always attaches to the confining potential for the same convention as Ref. [1], which can be fixed by the mass of the ground state.

In the literature, the following replacement is often employed to modify the linear confining potential in the quark model [57,58],

$$S(r) = br + c \to V^{scr}(r) = \frac{b(1-e^{-\mu r})}{\mu} + c. \tag{15}$$

If r is small enough, one has $V^{scr}(r) = V(r)$. Therefore, this replacement will minimally affect the ground states, and reduce the excited states significantly. The parameter μ is related to the strength of the screening effects, and one can roughly understand that the screening effects begin to work from $r \sim 1/\mu$. With the smearing transformation, one has

$$\tilde{V}^{scr}(r) = \frac{b}{\mu r}\left[e^{\frac{\mu^2}{4\sigma_{12}^2}+\mu r}\left(\frac{1}{\sqrt{\pi}}\int_0^{\frac{\mu+2r\sigma_{12}^2}{2\sigma_{12}}}e^{-x^2}dx - \frac{1}{2}\right)\times\frac{\mu+2r\sigma_{12}^2}{2\sigma_{12}^2} + r - e^{\frac{\mu^2}{4\sigma_{12}^2}-\mu r}\frac{\mu-2r\sigma_{12}^2}{2\sigma_{12}^2}\times\left(\frac{1}{\sqrt{\pi}}\int_0^{\frac{\mu-2r\sigma_{12}^2}{2\sigma_{12}}}e^{-x^2}dx - \frac{1}{2}\right)\right] + c. \tag{16}$$

Finally, by replacing the $\tilde{S}(r)$ with $\tilde{V}^{scr}$ in the original relativized quark model, we obtain the modified relativized quark model including the screening effects. The mass spectrum and wave functions of the mesons can be obtained by solving the relativized Hamiltonian, and the wave functions are used as inputs to investigate the subsequent strong decays for mesons.

C. The $^3P_0$ model

In addition to the mass spectrum, the decay widths are crucial to identify the assignments for mesons. Here, we give a brief introduction of the $^3P_0$ model which is widely used in studying two-body OZI-allowed strong decays of mesons [6,30,31,44,65–79]. In the $^3P_0$ model, the strong decay of a meson takes place by producing a quark-antiquark pair with vacuum quantum number $J^{PC} = 0^{++}$. The newly created quark-antiquark pair, together with the $q\bar{q}$ in the initial meson, regroups into two outgoing mesons in all possible quark rearrangements. Some detailed reviews on the $^3P_0$ model can be found in Refs. [67,68,72–74].

The transition operator T of the decay $A \to BC$ in the $^3P_0$ model is given by

$$T = -3\gamma \sum_m \langle 1, m; 1, -m|0, 0\rangle \int \mathrm{d}^3\boldsymbol{p}_3 \mathrm{d}^3\boldsymbol{p}_4 \delta^3(\boldsymbol{p}_3 + \boldsymbol{p}_4) \times \mathcal{Y}_1^m\left(\frac{\boldsymbol{p}_3 - \boldsymbol{p}_4}{2}\right)\chi^{34}_{1-m}\phi^{34}_0\omega^{34}_0 b^\dagger_3(\boldsymbol{p}_3)d^\dagger_4(\boldsymbol{p}_4), \quad (17)$$

where the γ is a dimensionless parameter denoting the production strength of the quark-antiquark pair $q_3\bar{q}_4$ with quantum number $J^{PC} = 0^{++}$. $\boldsymbol{p}_3$ and $\boldsymbol{p}_4$ are the momenta of the created quark q_3 and antiquark $\bar{q}_4$, respectively. $\chi^{34}_{1,-m}$, ϕ^{34}_0, and ω^{34}_0 are the spin, flavor, and color wave functions of $q_3\bar{q}_4$, respectively. The solid harmonic polynomial $\mathcal{Y}_1^m(\boldsymbol{p}) \equiv |\boldsymbol{p}|^1 Y_1^m(\theta_p, \phi_p)$ reflects the momentum-space distribution of the $q_3\overline{q_4}$.

The S matrix of the process $A \to BC$ is defined by

$$\langle BC|S|A\rangle = I - 2\pi i\delta(E_A - E_B - E_C)\langle BC|T|A\rangle, \quad (18)$$

where $|A\rangle$ ($|B\rangle$,$|C\rangle$) is the mock meson defined by [80]

$$|A(n_A^{2S_A+1}L_{A J_A M_{J_A}})(\boldsymbol{p}_A)\rangle \equiv \sqrt{2E_A}\sum_{M_{L_A},M_{S_A}} \langle L_A M_{L_A} S_A M_{S_A}|J_A M_{J_A}\rangle \times \int d^3\boldsymbol{p}_A \psi_{n_A L_A M_{L_A}}(\boldsymbol{p}_A)\chi^{12}_{S_A M_{S_A}}\phi^{12}_A\omega^{12}_A \times \left|q_1\left(\frac{m_1}{m_1+m_2}\boldsymbol{p}_A + \boldsymbol{p}_A\right)\bar{q}_2\left(\frac{m_2}{m_1+m_2}\boldsymbol{p}_A - \boldsymbol{p}_A\right)\right\rangle. \quad (19)$$

Here, m_1 and m_2 ($\boldsymbol{p}_1$ and $\boldsymbol{p}_2$) are the masses (momenta) of the quark q_1 and the antiquark $\bar{q}_2$, respectively; $\boldsymbol{p}_A = \boldsymbol{p}_1 + \boldsymbol{p}_2$, $\boldsymbol{p}_A = \frac{m_2\boldsymbol{p}_1 - m_1\boldsymbol{p}_2}{m_1+m_2}$; $\chi^{12}_{S_A M_{S_A}}$, ϕ^{12}_A, ω^{12}_A, and $\psi_{n_A L_A M_{L_A}}(\boldsymbol{p}_A)$ are the spin, flavor, color, and space wave functions of the meson A composed of $q_1\bar{q}_2$ with total energy E_A, respectively. n_A is the radial quantum number of the meson A. $\boldsymbol{S}_A = \boldsymbol{s}_{q_1} + \boldsymbol{s}_{\bar{q}_2}$, $\boldsymbol{J}_A = \boldsymbol{L}_A + \boldsymbol{S}_A$, $\boldsymbol{s}_{q_1}(\boldsymbol{s}_{\bar{q}_2})$ is the spin of $q_1(\bar{q}_2)$, and $\boldsymbol{L}_A$ is the relative orbital angular momentum between q_1 and $\bar{q}_2$.

The transition matrix element $\langle BC|T|A\rangle$ can be written as

$$\langle BC|T|A\rangle = \delta^3(\boldsymbol{p}_A - \boldsymbol{p}_B - \boldsymbol{p}_C)\mathcal{M}^{M_{J_A}M_{J_B}M_{J_C}}(\boldsymbol{p}), \quad (20)$$

where the helicity amplitude $\mathcal{M}^{M_{J_A}M_{J_B}M_{J_C}}(\boldsymbol{p})$ is

$$\mathcal{M}^{M_{J_A}M_{J_B}M_{J_C}}(\boldsymbol{p}) = \gamma\sqrt{8E_A E_B E_C}\sum_{M_{L_A},M_{S_A}}\sum_{M_{L_B},M_{S_B}}\sum_{M_{L_C},M_{S_C}}\sum_m \langle L_A M_{L_A} S_A M_{S_A}|J_A M_{J_A}\rangle \times \langle L_B M_{L_B} S_B M_{S_B}|J_B M_{J_B}\rangle\langle L_C M_{L_C} S_C M_{S_C}|J_C M_{J_C}\rangle \times \langle 1m1-m|00\rangle\langle\chi^{14}_{S_B M_{S_B}}\chi^{32}_{S_C M_{S_C}}|\chi^{12}_{S_A M_{S_A}}\chi^{34}_{1-m}\rangle \times [f_1 I(\boldsymbol{p}, m_1, m_2, m_3) + (-1)^{1+S_A+S_B+S_C} f_2 I(-\boldsymbol{p}, m_2, m_1, m_3)] \quad (21)$$

with $f_1 = \langle\phi^{14}_B\phi^{32}_C|\phi^{12}_A\phi^{34}_0\rangle$ and $f_2 = \langle\phi^{32}_B\phi^{14}_C|\phi^{12}_A\phi^{34}_0\rangle$, and

$$I(\boldsymbol{p}, m_1, m_2, m_3) = \int d^3\boldsymbol{p}\psi^*_{n_B L_B M_{L_B}}\left(\frac{m_3}{m_1+m_3}\boldsymbol{p}_B + \boldsymbol{p}\right) \times \psi^*_{n_C L_C M_{L_C}}\left(\frac{m_3}{m_2+m_3}\boldsymbol{p}_B + \boldsymbol{p}\right) \times \psi_{n_A L_A M_{L_A}}(\boldsymbol{p}_B + \boldsymbol{p})\mathcal{Y}_1^m(\boldsymbol{p}), \quad (22)$$

where $\boldsymbol{p} = \boldsymbol{p}_B = -\boldsymbol{p}_C$, $\boldsymbol{p} = \boldsymbol{p}_3$, m_3 is the mass of the created quark q_3. Also, the helicity amplitude can be transformed into the partial wave amplitude $\mathcal{M}^{LS}(\boldsymbol{p})$ [81],

$$\mathcal{M}^{LS}(\boldsymbol{p}) = \sum_{\substack{M_{J_B},M_{J_C},\\ M_S,M_L}} \langle L M_L S M_S|J_A M_{J_A}\rangle \times \langle J_B M_{J_B} J_C M_{J_C}|S M_S\rangle \times \int d\Omega Y^*_{LM_L}\mathcal{M}^{M_{J_A}M_{J_B}M_{J_C}}(\boldsymbol{p}). \quad (23)$$

Various $^3P_0$ models exist in literature and typically differ in the choices of the pair-production vertex, the phase space conventions, and the meson wave functions employed. In this work, we restrict to the simplest vertex as introduced originally by Micu [82] which assumes a spatially constant pair creation strength γ for the $u\bar{u}$ and $d\bar{d}$ pairs. For the $s\bar{s}$ pair, the creation strength is multiplied by a factor m_u/m_s.

The wave functions can be obtained from the modified relativized quark model including the screening effects. With the relativistic phase space, the decay width $\Gamma(A \to BC)$ can be expressed in terms of the partial wave amplitude

$$\Gamma(A \to BC) = \frac{\pi|\boldsymbol{p}|}{4M_A^2} \sum_{LS} |\mathcal{M}^{LS}(\boldsymbol{p})|^2, \tag{24}$$

where $|\boldsymbol{p}| = \sqrt{[M_A^2-(M_B+M_C)^2][M_A^2-(M_B-M_C)^2]}/2M_A$, and M_A, M_B, and M_C are the masses of the mesons A, B, and C, respectively.

III. CALCULATION AND RESULTS

A. Mass spectrum

The relevant parameters used in the original relativized quark model are listed in Table I [1]. When the screening effects are included, and extra parameter μ is introduced, which reflects the strength of screening effects. In the present work, we can get the parameter μ by reproducing the experimental data of low-lying states. As mentioned in the Introduction, seven states, D_s, D_s^*, $D_{s1}(2536)$, $D_{s2}^*(2573)$, $D_{s1}^*(2700)$, $D_{s1}^*(2860)$, and $D_{s3}^*(2860)$, can be reasonably classified in the conventional charmed-strange mesons. Since the $D_{s1}(2536)$ is a mixture of the $D_s(1^1P_1)$ and $D_s(1^3P_1)$ states, we do not include it when determining the parameter μ. Also, the overall constant c is readjusted by fixing the mass of $D_s(1^1S_0)$ to 1968 MeV when the μ varies.

TABLE I. Parameters in the Godfrey-Isgur's relativized quark model [1].

Parameter	Value	Parameter	Value	Parameter	Value
m_u (GeV)	0.22	b (GeV^2)	0.18	ϵ_c	−0.168
m_d (GeV)	0.22	c (GeV)	−0.253	ϵ_t	+0.025
m_s (GeV)	0.419	σ_0 (GeV)	1.8	$\epsilon_{so(v)}$	−0.035
m_c (GeV)	1.628	s	1.55	$\epsilon_{so(s)}$	+0.055

The mass spectrum of the charmed-strange meson with μ from 0.04 to 0.05 GeV is listed in Table II. For comparison, the experiment data and predictions of the original relativized quark model are also presented. It can be seen that the measured masses of the low-lying states can be well reproduced and the predicted spectrum in the screened potential is improved significantly. Moreover, we can estimate the corresponding χ^2 and present them in Table II. Here the χ^2 can be defined as

$$\chi^2 = \sum_i \left(\frac{\mathcal{A}_{\rm Th}(i) - \mathcal{A}_{\rm Exp}(i)}{\mathrm{Error}(i)} \right)^2, \tag{25}$$

where $\mathcal{A}_{\rm Th}(i)$, $\mathcal{A}_{\rm Exp}(i)$, and Error(i) are theoretical values, experimental values, and experimental errors, respectively. With the reasonable range of μ, the χ^2 of screened potential is significantly smaller than that of original relativized quark model.

It should be mentioned that the χ^2 is not the only criterion of the performances for different predictions in quark models. From Eq. (25), if the experimental accuracies of several states are high enough, the model with the smallest χ^2 may only reproduce these few states and fail to describe the whole mass spectrum. Phenomenologically, we also expect the absolute value $|\mathcal{A}_{\rm Th}(i) - \mathcal{A}_{\rm Exp}(i)|$ for each state is not too large, such that these states can be interpreted in the conventional $c\bar{s}$ picture. In the range of $\mu = 0.04$–0.05 GeV, the results meet the above requirements.

Hence, we prefer to choose $\mu = 0.045$ GeV to calculate the mass spectrum of charmed-strange mesons, and take the masses with $\mu = 0.04$ and 0.05 GeV as the theoretical uncertainties. With $\mu = 0.045$ GeV, one can obtain the constant c equals to −0.243. The theoretical predictions together with experimental data are shown in Fig. 1. It can be seen that the $D_{s0}(2590)^+$ can be assigned as the $D_s(2^1S_0)$ state according to its mass. Moreover, we compare the predictions of different models in Table III, and find that they give rather different

TABLE II. Comparison of the experimental data and theoretical results with different μ. We take $\mu = 0.04$, 0.045, 0.05 GeV to show the results with the modified relativized quark model with screened potential. We also list the χ^2 values for different models.

				Modified GI model		
	$n^{2S+1}L_J$	Experimental values	GI model	$\mu = 0.04$	$\mu = 0.045$	$\mu = 0.05$
$D_s^\pm$	1^1S_0	1968.34 ± 0.07	1979	1968	1968	1968
$D_s^{*\pm}$	1^3S_1	2112.2 ± 0.4	2129	2114	2114	2113
$D_{s2}^*(2573)$	1^3P_2	2569.1 ± 0.8	2592	2559	2556	2553
$D_{s1}^*(2700)^\pm$	2^3S_1	$2708^{+4.0}_{-3.4}$	2732	2681	2675	2670
$D_{s1}^*(2860)^\pm$	1^3D_1	$2859 \pm 12 \pm 24$	2899	2839	2833	2827
$D_{s3}^*(2860)^\pm$	1^3D_3	$2860.5 \pm 2.6 \pm 6.5$	2917	2858	2852	2846
χ^2			666	55.17	86.23	119.39

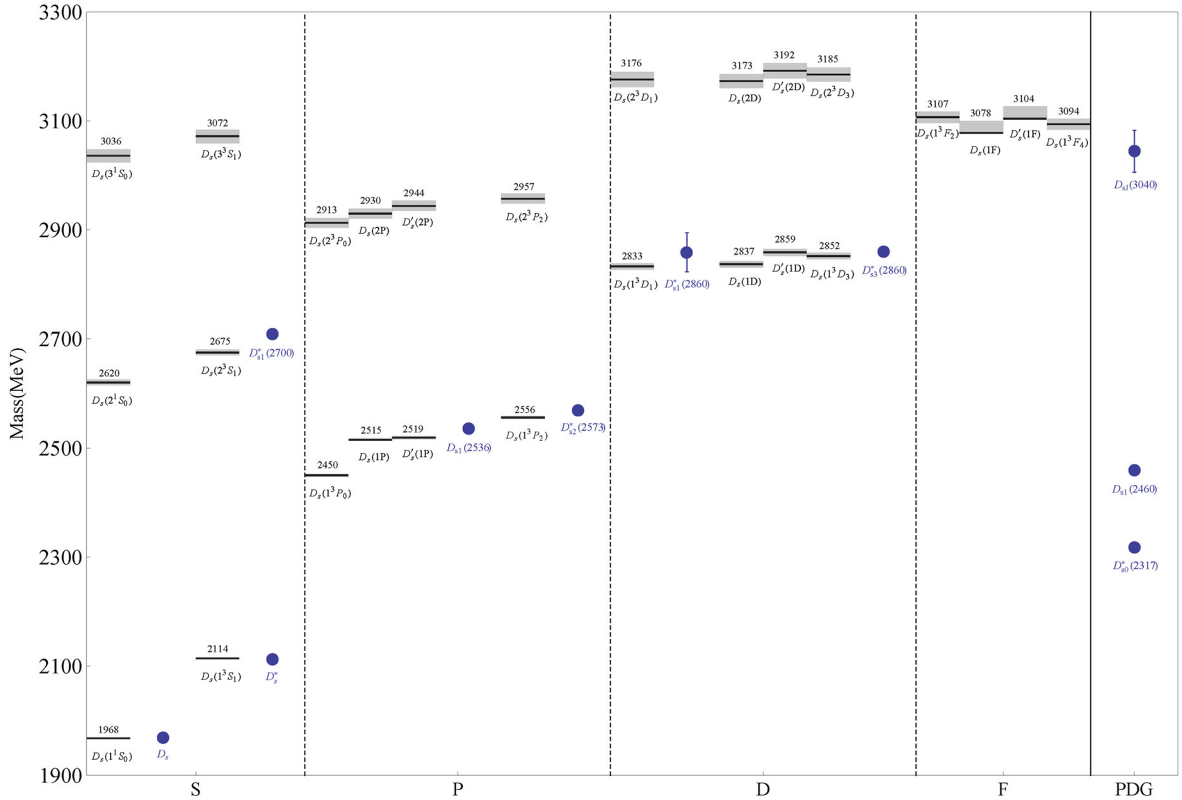

FIG. 1. Mass spectrum of the charmed-strange mesons in units of MeV. The black lines show the MGI model with $\mu = 0.045$ GeV and the shaded regions stand for the theoretical uncertainties with $\mu = 0.04$–0.05 GeV. The dark blue dots denote the experimental data [83] and the vertical lines represent the errors.

predictions for the higher states. Also, the screening effects become increasingly important as the masses go up. The information on highly excited states is crucial to distinguish these different models and test our screened potential.

B. Strong decays

Besides the mass spectrum, the strong decay behaviors are essential to clarify the internal structure of a new resonance. In this work, the $^3P_0$ model is adopted to investigate the strong decays of the $D_{s0}(2590)$. While we calculate the mass spectrum, the corresponding wave functions of mesons are also obtained. Then, only one parameter γ in the $^3P_0$ model needs to determine. We can assume that the charmed-strange mesons share the same γ, and fit this parameter from the known states. Among the seven reasonably classified states, D_s only decays though weak processes, D_s^* has no OZI-allowed strong decay, and the strong decays of $D_{s1}(2536)$ depend on the mixing angle sensitively. Hence, we adopt the remaining resonances, $D_{s2}^*(2573)$, $D_{s1}^*(2700)$, $D_{s1}^*(2860)$, and $D_{s3}^*(2860)$, to fit the parameter γ.

According to the fitting process, the $\gamma = 9.32$ is obtained, and the strong decay behaviors of the $D_{s2}^*(2573)$, $D_{s1}^*(2700)$, $D_{s1}^*(2860)$, and $D_{s3}^*(2860)$ are listed in Table IV. It can be seen that the calculated widths of $D_{s2}^*(2573)$ and $D_{s3}^*(2860)$ are consistent with the experimental data within errors, and the theoretical width of $D_{s1}^*(2700)$ and $D_{s1}^*(2860)$ seems a little bit larger. These differences may arise from the theoretical uncertainties of the $^3P_0$ model or the possible complicated $S-D$ mixing mechanism for the $D_{s1}^*(2700)$ and $D_{s1}^*(2860)$ states. Hence, with the $\gamma = 9.32$, the strong decay behaviors of these four states are fairly described. We employ this value to investigate the strong decays of $D_{s0}(2590)$.

The results of $D_{s0}(2590)$ as the $D_s(2^1S_0)$ state are listed in Table V. The calculated width is about 75 MeV, which agrees well with the experimental data $89 \pm 16 \pm 12$ MeV. Also, the dependence on the mass of initial state is shown in Fig. 2. When the mass of initial $D_s(2^1S_0)$ state varies from 2570 to 2610 MeV, the total width lies in the range of 51 to 98 MeV. Our results indicate that the $D_{s0}(2590)^+$ observed by LHC Collaboration can be interpreted as the conventional $D_s(2^1S_0)$ state.

TABLE III. Our predicted masses of charmed-strange mesons compared with the experimental data and other quark model predictions. The mixing angles of D_s–D_s' obtained in this work are $\theta_{1P} = -42.7°$, $\theta_{2P} = -31.4°$, $\theta_{1D} = -39.4°$, $\theta_{2D} = -38.4°$, $\theta_{1F} = -39.9°$. Horizontal lines indicate that the corresponding masses are not calculated in the references. The units are in MeV.

State	J^P	Ours	GI [1,7]	ZVR [2]	LNR [3]	DE [4]	EFG [5]	LJM [6]	NLZ [8]	Exp [83]
$D_s(1^1S_0)$	0^-	1968	1979	1940	1975	1965	1969	1969	1969	1968.34 ± 0.07
$D_s(1^3S_1)$	1^-	2114	2129	2130	2180	2113	2111	2107	2112	2112.2 ± 0.4
$D_s(2^1S_0)$	0^-	2620	2673	2610	2659	2700	2688	2640	2649	$2591 \pm 6 \pm 7$
$D_s(2^3S_1)$	1^-	2675	2732	2730	2722	2806	2731	2714	2737	$2708^{+4.0}_{-3.4}$
$D_s(3^1S_0)$	0^-	3072	3154	3090	3044	3259	3219	…	3126	…
$D_s(3^3S_1)$	1^-	3036	3193	3190	3087	3345	3242	…	3196	…
$D_s(1^3P_0)$	0^+	2450	2484	2380	2455	2487	2509	2344	2409	2317.8 ± 0.5
$D_s(1P)$	1^+	2515	2549	2510	2502	2535	2536	2488	2528	…
$D_s(1P')$	1^+	2519	2556	2520	2522	2605	2574	2510	2545	…
$D_s(1^3P_2)$	2^+	2556	2592	2580	2586	2581	2571	2559	2575	2569.1 ± 0.8
$D_s(2^3P_0)$	0^+	2913	3005	2900	2901	3067	3054	2830	2940	…
$D_s(2P)$	1^+	2930	3018	3000	2928	3114	3067	2958	3002	…
$D_s(2P')$	1^+	2944	3038	3010	2942	3165	3154	2995	3026	…
$D_s(2^3P_2)$	2^+	2957	3048	3060	2988	3157	3142	3040	3053	…
$D_s(1^3D_1)$	1^-	2833	2899	2820	2845	2913	2913	2804	2843	$2859 \pm 12 \pm 24$
$D_s(1D)$	2^-	2837	2900	2860	2838	2900	2931	2788	2851	…
$D_s(1D')$	2^-	2859	2926	2880	2856	2953	2961	2849	2911	…
$D_s(1^3D_3)$	3^-	2852	2917	2900	2857	2925	2971	2811	2882	$2860.5 \pm 2.6 \pm 6.5$
$D_s(2^3D_1)$	1^-	3176	3306	3250	3172	…	3383	3217	3233	…
$D_s(2D)$	2^-	3173	3298	3280	3144	…	3403	3217	3267	…
$D_s(2D')$	2^-	3192	3323	3290	3167	…	3456	3260	3306	…
$D_s(2^3D_3)$	3^-	3185	3311	3310	3157	…	3469	3240	3299	…
$D_s(1^3F_2)$	2^+	3107	3208	3120	…	3224	3230	…	3176	…
$D_s(1F)$	3^+	3078	3186	3130	…	…	3254	…	3123	…
$D_s(1F')$	3^+	3104	3218	3150	…	…	3266	…	3205	…
$D_s(1^3F_4)$	4^+	3094	3190	3160	…	3220	3300	…	3134	…

TABLE IV. Decay widths of $D_{s2}^*(2573)$, $D_{s1}^*(2700)^+$, $D_{s1}^*(2860)^+$ and $D_{s3}^*(2860)^+$ with fitted $\gamma = 9.32$ (in MeV).

Mode	$D_{s2}^*(2573)$	$D_{s1}^*(2700)^+$	$D_{s1}^*(2860)^+$	$D_{s3}^*(2860)^+$
DK	12.07	61.13	150.72	25.65
D^*K	1.27	116.05	76.36	17.27
DK^*	0.03	3.69	45.22	1.32
$D_s\eta$	…	1.61	10.78	0.52
$D_s^*\eta$	…	…	3.72	0.16
Total width	13.37	182.48	286.80	44.92
Experiment	16.9 ± 0.7	122 ± 10	$159 \pm 23 \pm 77$	$53 \pm 7 \pm 7$

TABLE V. Decay widths of $D_{s0}(2590)^+$ as the $D_s(2^1S_0)$ state with fitted $\gamma = 9.32$ (in MeV).

Mode	$D_{s0}(2590)^+$
$D^{*+}K^0$	35.52
$D^{*0}K^+$	39.38
Total width	74.90
Experiment	$89 \pm 16 \pm 12$

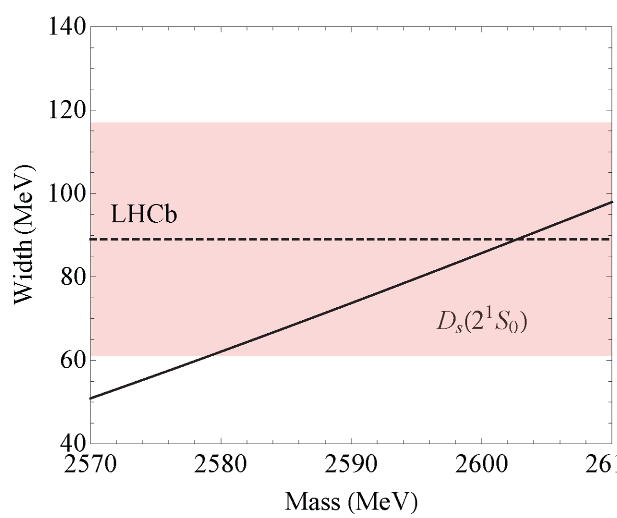

FIG. 2. The dependence of the total width of $D_s(2^1S_0)$ on the initial state mass.

IV. SUMMARY AND CONCLUSION

In this work, we investigate the mass spectrum of charmed-strange mesons with the modified relativized quark model including the screening effects. With reasonable strength of screening effects, the calculated mass spectrum can explain the $D_{s0}(2590)^+$ as well as other known charmed-strange mesons. The information on highly excited states is crucial to distinguish various predictions and test our results with screened potential.

Besides the mass spectrum, the strong decays of $D_{s0}(2590)^+$ as $D_s(2^1S_0)$ state are also investigated in the $^3P_0$ model with the obtained relativistic wave functions. The calculated width is about 75 MeV, which agrees well with the experimental data $89 \pm 16 \pm 12$ MeV. Our results indicate that the $D_{s0}(2590)^+$ can be interpreted as the conventional $D_s(2^1S_0)$ state.

Certainly, it is a tempting thought that describes the whole meson spectroscopy within one consistent set of parameters. As estimations, we also find that these parameters are suitable for the low-lying bottom and bottom-strange mesons owing to the heavy quark symmetry. However, to know accurately whether these parameters are suitable for other mesons, one should do systematic and tedious studies. Future investigations are needed to clarify this question.

ACKNOWLEDGMENTS

This work is partly supported by the China Postdoctoral Science Foundation Funded Project under Grant No. 2021M701086, and supported by the Natural Science Foundation of Henan under Grant No. 212300410123. It is also supported by the National Natural Science Foundation of China under Grant No. 11605123. Q.-F. L. is supported by the National Natural Science Foundation of China under Grants No. 11705056 and No. U1832173, by the Key Project of Hunan Provincial Education Department under Grant No. 21A0039, and by the State Scholarship Fund of China Scholarship Council under Grant No. 202006725011.

[1] S. Godfrey and N. Isgur, Mesons in a relativized quark model with chromodynamics, Phys. Rev. D **32**, 189 (1985).
[2] J. Zeng, J. W. Van Orden, and W. Roberts, Heavy mesons in a relativistic model, Phys. Rev. D **52**, 5229 (1995).
[3] T. A. Lahde, C. J. Nyfalt, and D. O. Riska, Spectra and M1 decay widths of heavy light mesons, Nucl. Phys. **A674**, 141 (2000).
[4] M. Di Pierro and E. Eichten, Excited heavy—light systems and hadronic transitions, Phys. Rev. D **64**, 114004 (2001).
[5] D. Ebert, R. N. Faustov, and V. O. Galkin, Heavy-light meson spectroscopy and Regge trajectories in the relativistic quark model, Eur. Phys. J. C **66**, 197 (2010).
[6] D. M. Li, P. F. Ji, and B. Ma, The newly observed open-charm states in quark model, Eur. Phys. J. C **71**, 1582 (2011).
[7] S. Godfrey and K. Moats, Properties of excited charm and charm-strange mesons, Phys. Rev. D **93**, 034035 (2016).
[8] R. H. Ni, Q. Li, and X. H. Zhong, Mass spectra and strong decays of charmed and charmed-strange mesons, Phys. Rev. D **105**, 056006 (2022).
[9] P. Colangelo, F. De Fazio, F. Giannuzzi, and S. Nicotri, New meson spectroscopy with open charm and beauty, Phys. Rev. D **86**, 054024 (2012).
[10] S. Campanella, P. Colangelo, and F. De Fazio, Excited heavy meson decays to light vector mesons: Implications for spectroscopy, Phys. Rev. D **98**, 114028 (2018).
[11] P. Colangelo and F. De Fazio, Understanding $D_{sJ}(2317)$, Phys. Lett. B **570**, 180 (2003).
[12] G. L. Wang, W. Li, T. F. Feng, Y. L. Wang, and Y. B. Liu, The newly observed state $D_{s0}(2590)^+$ and width of $D^*(2007)^0$, Eur. Phys. J. C **82**, 267 (2022).
[13] J. M. Xie, M. Z. Liu, and L. S. Geng, $D_{s0}(2590)$ as a dominant $c\bar{s}$ state with a small D^*K component, Phys. Rev. D **104**, 094051 (2021).
[14] P. G. Ortega, J. Segovia, D. R. Entem, and F. Fernandez, The $D_{s0}(2590)^+$ as the dressed $c\bar{s}(2^1S_0)$ meson in a coupled-channels calculation, Phys. Lett. B **827**, 136998 (2022).
[15] Y. Tan and J. Ping, $D^*_{s0}(2317)$ and $D_{s1}(2460)$ in an unquenched quark model, arXiv:2111.04677.
[16] T. E. Browder, S. Pakvasa, and A. A. Petrov, Comment on the new $D_s^{(*)+}\pi^0$ resonances, Phys. Lett. B **578**, 365 (2004).
[17] D. S. Hwang and D. W. Kim, Mass shift of $D^*_{sJ}(2317)$ by coupled channel effect, J. Phys. Conf. Ser. **9**, 63 (2005).
[18] J. Lu, X. L. Chen, W. Z. Deng, and S. L. Zhu, Pionic decays of $D_{sj}(2317)$, $D_{sj}(2460)$ and $B_{sj}(5718)$, $B_{sj}(5765)$, Phys. Rev. D **73**, 054012 (2006).
[19] P. Bicudo, Confining quark-model suggestion against $D^*_s(2317)$ and $D^*_s(2460)$ as chiral partners of standard D_s, Phys. Rev. D **74**, 036008 (2006).
[20] D. Mohler and R. M. Woloshyn, D and D_s meson spectroscopy, Phys. Rev. D **84**, 054505 (2011).
[21] A. Martinez Torres, L. R. Dai, C. Koren, D. Jido, and E. Oset, KD, ηD_s interaction in finite volume and the $D_{s^*0}(2317)$ resonance, Phys. Rev. D **85**, 014027 (2012).
[22] D. Mohler, C. B. Lang, L. Leskovec, S. Prelovsek, and R. M. Woloshyn, $D^*_{s0}(2317)$ Meson and D-Meson-Kaon Scattering from Lattice QCD, Phys. Rev. Lett. **111**, 222001 (2013).
[23] C. B. Lang, L. Leskovec, D. Mohler, S. Prelovsek, and R. M. Woloshyn, D_s mesons with DK and D^*K scattering near threshold, Phys. Rev. D **90**, 034510 (2014).

[24] P. G. Ortega, J. Segovia, D. R. Entem, and F. Fernandez, Molecular components in P-wave charmed-strange mesons, Phys. Rev. D **94**, 074037 (2016).

[25] A. Martínez Torres, E. Oset, S. Prelovsek, and A. Ramos, An analysis of the lattice QCD spectra for $D_{s0}^*(2317)$ and $D_{s1}^*(2460)$, *Proc. Sci.*, Hadron2017 (2018) 024 [arXiv: 1712.09468].

[26] G. S. Bali, S. Collins, A. Cox, and A. Schäfer, Masses and decay constants of the $D_{s0}^*(2317)$ and $D_{s1}(2460)$ from $N_f = 2$ lattice QCD close to the physical point, Phys. Rev. D **96**, 074501 (2017).

[27] M. Albaladejo, P. Fernandez-Soler, J. Nieves, and P. G. Ortega, Contribution of constituent quark model $c\bar{s}$ states to the dynamics of the $D_{s0}^*(2317)$ and $D_{s1}(2460)$ resonances, Eur. Phys. J. C **78**, 722 (2018).

[28] S. Godfrey and K. Moats, The $D_{sJ}^*(2860)$ mesons as excited D-wave $c\bar{s}$ states, Phys. Rev. D **90**, 117501 (2014).

[29] Q. T. Song, D. Y. Chen, X. Liu, and T. Matsuki, Charmed-strange mesons revisited: Mass spectra and strong decays, Phys. Rev. D **91**, 054031 (2015).

[30] B. Zhang, X. Liu, W. Z. Deng, and S. L. Zhu, $D_{sJ}(2860)$ and $D_{sJ}(2715)$, Eur. Phys. J. C **50**, 617 (2007).

[31] D. M. Li and B. Ma, Implication of *BABAR*'s new data on the $D_{s1}(2710)$ and $D_{sJ}(2860)$, Phys. Rev. D **81**, 014021 (2010).

[32] B. Aubert *et al.* (*BABAR* Collaboration), Observation of a Narrow Meson Decaying to $D_s^+\pi^0$ at a Mass of 2.32 GeV/c^2, Phys. Rev. Lett. **90**, 242001 (2003).

[33] D. Besson *et al.* (CLEO Collaboration), Observation of a narrow resonance of mass 2.46 GeV/c^2 decaying to $D_s^{*+}\pi^0$ and confirmation of the $D_{sJ}^*(2317)$ state, Phys. Rev. D **68**, 032002 (2003).

[34] Particle Data Group (2021), https://pdg.lbl.gov/.

[35] R. Aaij *et al.* (LHCb Collaboration), Amplitude analysis of the $B^+ \to D^+D^-K^+$ decay, Phys. Rev. D **102**, 112003 (2020).

[36] R. Aaij *et al.* (LHCb Collaboration), A Model-Independent Study of Resonant Structure in $B^+ \to D^+D^-K^+$ Decays, Phys. Rev. Lett. **125**, 242001 (2020).

[37] R. Aaij *et al.* (LHCb Collaboration), Observation of a New Excited D_s^+ Meson in $B^0 \to D^-D^+K^+\pi^-$ Decays, Phys. Rev. Lett. **126**, 122002 (2021).

[38] R. Aaij *et al.* (LHCb Collaboration), Determination of quantum numbers for several excited charmed mesons observed in $B^- \to D^{*+}\pi^-\pi^-$ decays, Phys. Rev. D **101**, 032005 (2020).

[39] Y. S. Li, X. Liu, and F. S. Yu, Revisiting semileptonic decays of $\Lambda_{b(c)}$ supported by baryon spectroscopy, Phys. Rev. D **104**, 013005 (2021).

[40] S. Godfrey, Spectroscopy of B_c mesons in the relativized quark model, Phys. Rev. D **70**, 054017 (2004).

[41] S. Capstick and N. Isgur, Baryons in a relativized quark model with chromodynamics, Phys. Rev. D **34**, 2809 (1986).

[42] Y. Sun, Q. T. Song, D. Y. Chen, X. Liu, and S. L. Zhu, Higher bottom and bottom-strange mesons, Phys. Rev. D **89**, 054026 (2014).

[43] S. Godfrey, K. Moats, and E. S. Swanson, B and B_s meson spectroscopy, Phys. Rev. D **94**, 054025 (2016).

[44] T. Barnes, S. Godfrey, and E. S. Swanson, Higher charmonia, Phys. Rev. D **72**, 054026 (2005).

[45] Q. F. Lü, D. Y. Chen, Y. B. Dong, and E. Santopinto, Triply-heavy tetraquarks in an extended relativized quark model, Phys. Rev. D **104**, 054026 (2021).

[46] Q. F. Lü, D. Y. Chen, and Y. B. Dong, Masses of fully heavy tetraquarks $QQ\bar{Q}\bar{Q}$ in an extended relativized quark model, Eur. Phys. J. C **80**, 871 (2020).

[47] Q. F. Lü, D. Y. Chen, and Y. B. Dong, Masses of doubly heavy tetraquarks $T_{QQ'}$ in a relativized quark model, Phys. Rev. D **102**, 034012 (2020).

[48] Q. F. Lü, D. Y. Chen, and Y. B. Dong, Open charm and bottom tetraquarks in an extended relativized quark model, Phys. Rev. D **102**, 074021 (2020).

[49] Q. F. Lü and Y. B. Dong, X(4140), X(4274), X(4500), and X (4700) in the relativized quark model, Phys. Rev. D **94**, 074007 (2016).

[50] Q. F. Lü and Y. B. Dong, Masses of open charm and bottom tetraquark states in a relativized quark model, Phys. Rev. D **94**, 094041 (2016).

[51] Q. F. Lü, K. L. Wang, and Y. B. Dong, The $ss\bar{s}\,\bar{s}$ tetraquark states and the newly observed structure $X(2239)$ by BESIII Collaboration, Chin. Phys. C **44**, 024101 (2020).

[52] M. N. Anwar, J. Ferretti, F. K. Guo, E. Santopinto, and B. S. Zou, Spectroscopy and decays of the fully-heavy tetraquarks, Eur. Phys. J. C **78**, 647 (2018).

[53] M. N. Anwar, J. Ferretti, and E. Santopinto, Spectroscopy of the hidden-charm $[qc][\bar{q}\,\bar{c}]$ and $[sc][\bar{s}\,\bar{c}]$ tetraquarks in the relativized diquark model, Phys. Rev. D **98**, 094015 (2018).

[54] M. A. Bedolla, J. Ferretti, C. D. Roberts, and E. Santopinto, Spectrum of fully-heavy tetraquarks from a diquark + antidiquark perspective, Eur. Phys. J. C **80**, 1004 (2020).

[55] J. Ferretti and E. Santopinto, Hidden-charm and bottom tetra- and pentaquarks with strangeness in the hadro-quarkonium and compact tetraquark models, J. High Energy Phys. 04 (2020) 119.

[56] B. Q. Li and K. T. Chao, Higher charmonia and X,Y,Z states with screened potential, Phys. Rev. D **79**, 094004 (2009).

[57] K. T. Chao, Y. B. Ding, and D. H. Qin, Possible phenomenological indication for the string Coulomb term and the color screening effects in the quark—anti-quark potential, Commun. Theor. Phys. **18**, 321 (1992).

[58] Y. B. Ding, K. T. Chao, and D. H. Qin, Screened Q anti-Q potential and spectrum of heavy quarkonium, Chin. Phys. Lett. **10**, 460 (1993).

[59] Q. T. Song, D. Y. Chen, X. Liu, and T. Matsuki, Higher radial and orbital excitations in the charmed meson family, Phys. Rev. D **92**, 074011 (2015).

[60] J. Z. Wang, Z. F. Sun, X. Liu, and T. Matsuki, Higher bottomonium zoo, Eur. Phys. J. C **78**, 915 (2018).

[61] C. Q. Pang, J. Z. Wang, X. Liu, and T. Matsuki, A systematic study of mass spectra and strong decay of strange mesons, Eur. Phys. J. C **77**, 861 (2017).

[62] C. Q. Pang, Excited states of ϕ meson, Phys. Rev. D **99**, 074015 (2019).

[63] C. Q. Pang, Y. R. Wang, and C. H. Wang, Prediction for 5^{++} mesons, Phys. Rev. D **99**, 014022 (2019).

[64] W. Hao, G. Y. Wang, E. Wang, G. N. Li, and D. M. Li, Canonical interpretation of the $X(4140)$ state within the $^3P_0$ model, Eur. Phys. J. C **80**, 626 (2020).

[65] T. Barnes, N. Black, and P. R. Page, Strong decays of strange quarkonia, Phys. Rev. D **68**, 054014 (2003).
[66] G. Y. Wang, S. C. Xue, G. N. Li, E. Wang, and D. M. Li, Strong decays of the higher isovector scalar mesons, Phys. Rev. D **97**, 034030 (2018).
[67] W. Roberts and B. Silvestre-Brac, General method of calculation of any hadronic decay in the $^3P_0$ triplet model, Few-Body Syst. **11**, 171 (1992).
[68] H. G. Blundell, Meson properties in the quark model: A look at some outstanding problems, arXiv:hep-ph/9608473.
[69] T. Barnes, F. E. Close, P. R. Page, and E. S. Swanson, Higher quarkonia, Phys. Rev. D **55**, 4157 (1997).
[70] F. E. Close and E. S. Swanson, Dynamics and decay of heavy-light hadrons, Phys. Rev. D **72**, 094004 (2005).
[71] G. J. Ding and M. L. Yan, $Y(2175)$: Distinguish hybrid state from higher quarkonium, Phys. Lett. B **657**, 49 (2007).
[72] D. M. Li and B. Ma, $X(1835)$ and $\eta(1760)$ observed by the BES Collaboration, Phys. Rev. D **77**, 074004 (2008).
[73] D. M. Li and B. Ma, The $\eta(2225)$ observed by the BES Collaboration, Phys. Rev. D **77**, 094021 (2008).
[74] D. M. Li and S. Zhou, Towards the assignment for the 4^1S_0 meson nonet, Phys. Rev. D **78**, 054013 (2008).
[75] D. M. Li and S. Zhou, Nature of the $\pi_2(1880)$, Phys. Rev. D **79**, 014014 (2009).
[76] D. M. Li and E. Wang, Canonical interpretation of the $\eta_2(1870)$, Eur. Phys. J. C **63**, 297 (2009).
[77] Q. F. Lü and D. M. Li, Understanding the charmed states recently observed by the LHCb and *BABAR* Collaborations in the quark model, Phys. Rev. D **90**, 054024 (2014).
[78] T. T. Pan, Q. F. Lü, E. Wang, and D. M. Li, Strong decays of the $X(2500)$ newly observed by the BESIII Collaboration, Phys. Rev. D **94**, 054030 (2016).
[79] Q. F. Lü, T. T. Pan, Y. Y. Wang, E. Wang, and D. M. Li, Excited bottom and bottom-strange mesons in the quark model, Phys. Rev. D **94**, 074012 (2016).
[80] C. Hayne and N. Isgur, Beyond the wave function at the origin: Some momentum-dependent effects in the non-relativistic quark model, Phys. Rev. D **25**, 1944 (1982).
[81] M. Jacob and G. C. Wick, On the general theory of collisions for particles with spin, Ann. Phys. (N.Y.) **7**, 404 (1959).
[82] L. Micu, Decay rates of meson resonances in a quark model, Nucl. Phys. **B10**, 521 (1969).
[83] P. A. Zyla *et al.* (Particle Data Group), Review of particle physics, Prog. Theor. Exp. Phys. **2020**, 083C01 (2020).